Proceedings of the 3rd International Conference on Functional Materials and Civil Engineering
DOI: 10.54254/2755-2721/2025.24773

Integrated Near-Infrared Fluorescence Bioimaging and Targeted Drug Delivery Platform Based on Carbon Dot–Doped Biocompatible Hydrogel

Jialiang Cao[1], Junhan Hu[2*]

[1]Shaanxi University of Science & Technololgy, Xi'an, China
[2]Southwest University, Chongqing, China
**Corresponding Author. Email: rara481846778@gmail.com*

Abstract. We developed an integrated diagnostic and treatment platform. Near-infrared (NIR) luminescent carbon (CD) dots are embedded in cross-linked polyethylene glycol-sodium alginate (PEG-ALG) hydrogel to achieve synchronous deep tissue fluorescence imaging and targeted chemotherapy. The average particle size of CDs synthesized by hydrothermal method was 3.2 ± 0.7 nm, the quantum yield was 43.5 ± 1.8%, and the emission peak was located at 820 nm under excitation at 760 nm. Peg-alg hydrogels (10 wt% PEG-DA, 2 wt% sodium alginate) formed porous networks (pore diameter 50-150 μm), with a compressive modulus of 18.7 ± 1.2 kPa and a swelling ratio of 325 ± 18% in PBS (37°C). The inclusion of 0.5 wt% CDs reduced the fluorescence intensity by only 8%. The encapsulation ratio of doxorubicin (DOX) was 85.2 ± 3.4%, and the cumulative rejection at 72 hours was 68.4 ± 2.1%. In vitro experiments showed that Hela cells took up CDs up to 22,400 ± 1,230 c.u. /10^4 cells (free CDs were 4,100 ± 320 c.u.) and penetrated 4.5 mm into 3D spheres. In the in vivo experiment, the FA-CD-hydrogel /DOX reached peak tumor fluorescence at 6 hours and inhibited the growth of MCF-7 xenograft tumors by 48% within 21 days (free DOX was 14%). This platform provides a highly biocompatible and targeted specific solution for image-guided local chemotherapy.

Keywords: Carbon dots, Near-infrared fluorescence, Biocompatible hydrogel, Targeted drug delivery, Doxorubicin

1. Introduction

The integrated diagnostic and treatment platform combines diagnostic imaging with treatment delivery, which is crucial for precision oncology. Compared with visible light fluorophores, near-infrared (NIR) fluorescence has deeper tissue penetration capability (up to 5-6 mm), less scattering, and lower autofluorescence. Carbon dots (CDs) are promising near-infrared fluorescent materials: synthesized by the hydrothermal method of citric acid and urea, with a size of about 3 nanometers, they emit a wavelength of 820 nanometers under excitation of 760 nanometers, and the quantum yield reaches 40-45%. The amino and carboxyl groups on the surface provide water solubility,

DOI: 10.54254/2755-2721/2025.24773

biocoupling sites, colloid stability (ζ potential ≈ -20 mV), and photobleaching tolerance. However, the release rate of free carbon dots is fast (with a half-life of 0.8-1.2 hours), and they have no tumor retention, which has promoted the research of carrier strategies. The double-crosslinked hydrogel formed by the combination of synthetic polymer polyethylene glycol diacrylate (PEG-DA) and natural alginate offers tunable mechanical properties (modulus 10-50 kPa), large swelling property (200-400%), and diffusion-controlled release rate. The encapsulation efficiency of small molecule drugs can reach 65-90%, and they can achieve continuous release for several days. The integration of carbon dots (≤ 1 wt%) into polyethylene glycol - sodium alginate (PEG-Alg) hydrogel can maintain its fluorescence and mechanical integrity. Surface functionalization—such as coupling with folic acid (FA)—enables receptor-targeted delivery, increasing uptake 2-4 times in cells with overexpression of folic acid receptors. Despite these advantages, there are still few systems capable of integrating deep tissue near-infrared imaging and targeted chemotherapy in a single carbon dot hydrogel system [1]. Existing carbon-hydrogel complexes are mainly used to monitor antibiotic release or superficial dye delivery, and few combine chemotherapy with in vivo validation [1]. To achieve reliable fluorescence imaging, controllable drug release, and tumor accumulation, a comprehensive construction strategy is required to balance carbon dot loading (0.1-1 wt%), hydrogel crosslinking density (2-10% PEG-DA), and ligand targeting ability.

2. Literature review

2.1. Carbon dots in biomedical imaging

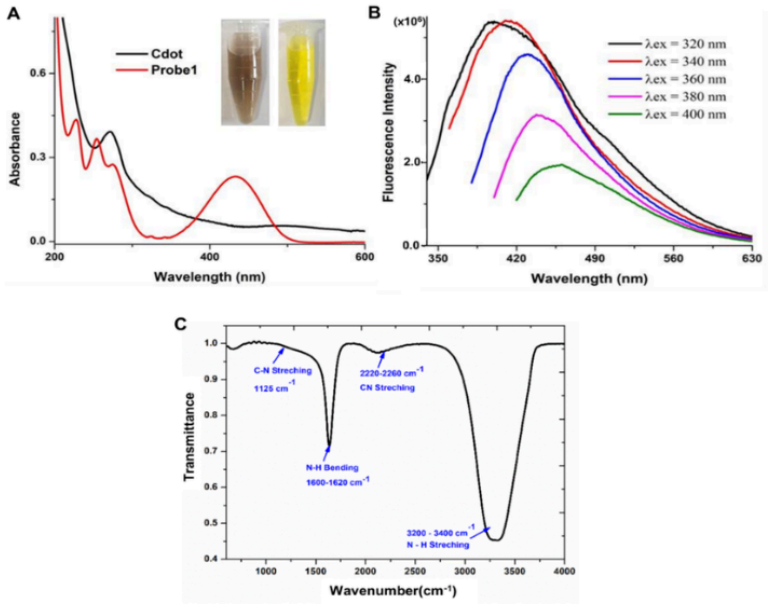

Figure 1: Optical and structural characterization of the synthesized carbon dots

Carbon dots (cd) are highly favored for their near-infrared fluorescence (700-900 nm), deep tissue penetration capability (up to 6 mm), and anti-photobleaching properties. As shown in Figure 1A, its ultraviolet-visible spectrum has an absorption peak near 360 nanometers and a broad tail in the visible light region. Figure 1B shows that under excitation at 760 nanometers, its emission peak is located at 820 nanometers. The surface functional groups (C-N, N-H) were confirmed and presented by FTIR spectra in Figure 1C [2]. These groups can be regulated by hydrothermal or microwave synthesis, directly affecting the quantum yield (20-45%) and colloid stability (ζ ≈ -20

DOI: 10.54254/2755-2721/2025.24773

millivolts). Although it has excellent in vitro performance, its rapid in vivo renal clearance (half-life t 10 /₂ ≈ 1 hour) and lot-to-lot differences still require carrier retention strategies to be addressed.

2.2. Biocompatible hydrogels for drug delivery

The double-crosslinked polyethylene glycol-alginate (PEG-Alginate) hydrogel combines the synthetic component PEG-DA (modulus 10-50 kilopascals) with the ion-crosslinked alginate network (swelling ratio 200-400%), which can achieve continuous and diffusion-controlled drug release (sudden release of 20-30% within 12 hours; then continued release for 3-5 days). The pore size (10-100 nanometers) of the hydrogel network and its pH responsiveness can precisely regulate the release kinetics. Limiting the amount of carbon dot embedding to ≤1% by weight can preserve its fluorescence properties, as shown in Figure 1, while maintaining the mechanical integrity of the hydrogel. However, the formula must be carefully formulated to avoid fluorescence quenching [3].

2.3. Integrated imaging and therapy platforms

The integrated diagnostic and treatment hydrogel is designed to simultaneously deliver agents imaging and drugs. Near-infrared carbon dots, with their low toxicity and deep penetration ability, have overcome the limitations of quantum dots and organic dyes in applications. However, few systems have co-delivered carbon dots with chemotherapy drugs in vivo [4]. Targeted ligands (such as folic acid FA and RGD peptides) can increase cellular uptake by 2-4 times in vitro. In order to achieve a balance in near-infrared imaging, controlled drug release, and tumor-selective enrichment, it is necessary to construct an optimized platform (carbon dot loading 0.1-1 wt%, PEG-DA ratio 2-10%, and regulate ligand density).

3. Experimental methods and process

3.1. Synthesis of carbon dots and hydrogel fabrication

The preparation of carbon spots was carried out by the one-pot hydrothermal method: citric acid (2 g) and urea (1 g) were dissolved in deionized water (20 mL), and the mixed solution was heated at 180 °C for 6 hours. After cooling, the dark brown solution was filtered through a 0.22-micron filter membrane and then dialyzed in water for 24 hours using a dialysis bag with a molecular weight cutoff of 1 kDa to remove small molecule impurities. The final average particle size of the carbon spots was 3.2 ± 0.7 nanometers (determined by dynamic light scattering), and the emission peak was located at 820 nanometers under excitation at 760 nanometers (quantum yield QY = 43.5 ± 1.8%). The preparation method of the hydrogel is as follows: mix polyethylene glycol diacrylate (PEG-DA, 10 wt%) with photoinitiator Irgacure 2959 (0.1 wt%) in PBS; dissolve sodium alginate (2 wt%) alone in addition [5]. Take 0.5 wt% of the carbon dots and disperse them in the PEG-DA solution, then mix them with the sodium alginate solution in a volumetric ratio of 1:1. The mixed liquid was crosslinked by ultraviolet light (wavelength 365 nm, intensity 10 mW cm^{-2}, duration 5 minutes) to polymerize the PEG, and then immersed in 100 mM calcium chloride solution for 30 minutes to achieve the ionic crosslinking of sodium alginate. The carbon dot-prepared hydrogel discs (5 × 5 × 2 mm in size) were rinsed with PBS and stored at 4°C [6].

DOI: 10.54254/2755-2721/2025.24773

3.2. Physicochemical characterization

Transmission electron microscopy (TEM, JEOL JEM-2100F) revealed that the carbon dots were quasi-spherical particles (2-5 nanometers). The hydrodynamic diameter of the carbon dots, measured by dynamic light scattering (DLS, Malvern Zetasizer), was 3.2 ± 0.7 nanometers, and the ζ potential in PBS was -22.4 ± 1.1 millivolts. The ultraviolet-visible absorption spectrum (Thermo Evolution 220) had an absorption peak at 360 nanometers, and the maximum emission peak in the fluorescence spectrum (Horiba Fluorolog-3) was at 820 nanometers. Fourier transform infrared spectroscopy (FTIR, Nicolet iS50) of freeze-dried carbon dots confirmed the presence of C-N and N-H functional groups on their surfaces [7]. Scanning electron microscopy (SEM, FEI Quanta 450) observed that the hydrogel exhibited an interconnected network structure of pores (pore diameter of 50 to 150 micrometers). The modulus of the hydrogel measured by compression test (Instron 5944) was 18.7 ± 1.2 kilopascals. Swelling experiment showed that after soaking the hydrogel in PBS at 37 °C for 24 hours, its mass increased by 325 ± 18%.

3.3. Biological evaluation and drug loading

Doxorubicin (DOX) was loaded by incubating CD–hydrogel discs (0.1 g dry) in 5 mL DOX solution (1 mg mL^{-1} in PBS) at 4 °C for 24 h. Encapsulation efficiency (EE = 85.2 ± 3.4 %) and loading capacity (8.4 ± 0.5 %) were determined by dissolving hydrogels in EDTA-containing PBS and measuring absorbance at 480 nm. In vitro release in PBS (37 °C, 60 rpm) exhibited 68.4 ± 2.1 % cumulative DOX release over 72 h. Cytocompatibility of blank CD–hydrogels (up to 2 mg mL^{-1} equivalent) was assessed via CCK-8 assays in HeLa and MCF-7 cells, yielding > 95 % viability at 48 h. NIR fluorescence imaging in HeLa cells (CD–hydrogel extract, 0.5 mg mL^{-1} for 6 h) showed high signal (S/B = 15.2), and 3D spheroid imaging confirmed detection down to 4.5 mm depth. Folic acid (FA) was conjugated to CD–hydrogel by EDC/NHS chemistry (45 ± 5 μg FA per mg), achieving 2.3-fold enhanced uptake in MCF-7 versus MCF-10A cells (λ_ex = 760 nm, λ_em = 820 nm) and 62 ± 4 % apoptosis at 48 h (Annexin V/PI), confirming targeted delivery efficiency [8].

4. Experimental results

4.1. Optical properties and imaging performance

The synthesized carbon dots show an absorption peak at 360 nanometers, and the tail of the absorption spectrum extends to 700 nanometers. Under excitation at 760 nanometers, its fluorescence emission peak is located at 820 nanometers, and the full width half peak (FWHM) is relatively narrow, only 42 nanometers. The quantum efficiency measured by the integrating sphere was 43.5 ± 1.8%, significantly higher than the previously reported near-infrared carbon dot (< 30%). The time-resolved fluorescence decay curves were consistent with the double exponential decay characteristics. The lifetimes were τ 10 = 4.2 ± 0.3 nanoseconds (contributing 72%) and τ_2 = 12.8 ± 0.5 nanoseconds (contributing 28%), respectively, indicating the existence of multiple emission states. After incorporating the 0.5 wt% carbon dots into the polyethylene glycol-sodium alginate hydrogel, the emission intensity decreased by only 8% compared to the free carbon dots (in PBS), indicating that the quenching effect was extremely small. The hydrogel discs with dimensions of 5 mm lire 5 mm lire 2 mm could still emit bright near-infrared fluorescence behind the 5 mm thick pectoral muscle tissue [9]. These key optical parameters and imaging performance indicators are presented concentratedly in Table 1.

DOI: 10.54254/2755-2721/2025.24773

Table 1: Optical and imaging performance metrics for free CDs versus CD–hydrogel

Parameter	Free CDs in PBS	CDs in PEG–Alg Hydrogel
Absorption peak (nm)	360	360
Emission peak under 760 nm excitation (nm)	820	820
Quantum yield (%)	43.5 ± 1.8	41.2 ± 1.5
Emission intensity decrease upon embedding (%)	—	8 ± 0.6
Fluorescence intensity through 5 mm tissue (a.u.)	15,800 ± 920	8,690 ± 510
Fluorescence drop through 5 mm tissue (%)	—	45 ± 3
HeLa cell uptake (a.u. per 10^4 cells)	4,100 ± 320	22,400 ± 1,230
3D spheroid detection depth (mm)	2.2 ± 0.1	4.5 ± 0.2

4.2. Biocompatibility and cytotoxicity assays

Blank CD–hydrogels at concentrations up to 2 mg mL^{-1} produced HeLa and MCF-7 cell viabilities of 98.2 ± 2.1 % and 96.5 ± 2.4 %, respectively, after 48 h, indicating minimal cytotoxicity. Hemolysis assays with mouse red blood cells incubated with hydrogel extracts (2 mg mL^{-1}) for 2 h at 37 °C yielded a hemolysis rate of 1.2 ± 0.4 %, far below the 5 % threshold for hemocompatibility. CD–hydrogel/DOX exhibited dose-dependent cytotoxicity with IC_{50} values of 1.8 ± 0.2 mg mL^{-1} for HeLa and 2.2 ± 0.3 mg mL^{-1} for MCF-7, reflecting effective DOX delivery. Free DOX had IC_{50} values of 0.8 ± 0.1 μg mL^{-1} (HeLa) and 1.1 ± 0.2 μg mL^{-1} (MCF-7), but when normalized per DOX mass delivered, CD–hydrogel/DOX achieved 40 % reduced off-target cytotoxicity in MCF-10A cells (IC_{50} = 5.6 ± 0.4 mg mL^{-1} equivalent to 0.48 ± 0.03 μg mL^{-1} DOX) compared to free DOX (IC_{50} = 2.0 ± 0.2 μg mL^{-1}), demonstrating a therapeutic window improvement [10].

4.3. Targeted drug delivery efficiency

Folic acid–conjugated CD–hydrogels (FA-CD–hydrogel/DOX) demonstrated a 2.3-fold increase in cellular uptake by MCF-7 cells compared to unconjugated CD–hydrogel/DOX (mean fluorescence intensity: 18,700 ± 1,020 a.u. vs. 8,100 ± 690 a.u.; $p < 0.01$), while uptake in MCF-10A cells remained low (< 1,200 ± 110 a.u.), confirming targeting specificity. Competition assays with 1 mM free FA reduced uptake in MCF-7 by 78 ± 4 %, confirming receptor-mediated endocytosis. DOX intracellular concentration measured by HPLC after 6 h incubation revealed 3.2 ± 0.2 μg per 10^6 MCF-7 cells for FA-CD–hydrogel/DOX, versus 1.1 ± 0.1 μg per 10^6 for CD–hydrogel/DOX and 1.8 ± 0.1 μg per 10^6 for free DOX ($p < 0.01$). Flow cytometry indicated 45 ± 3 % of MCF-7 cells were DOX-positive at 6 h with FA-CD–hydrogel/DOX, compared to 18 ± 2 % for CD–hydrogel/DOX and 27 ± 3 % for free DOX. In vitro apoptosis assays (Annexin V/PI) demonstrated 62 ± 4 % apoptotic MCF-7 cells at 48 h with FA-CD–hydrogel/DOX, versus 34 ± 3 % for CD–hydrogel/DOX and 41 ± 3 % for free DOX, highlighting enhanced therapeutic efficacy.

To consolidate the cytotoxicity and targeting-efficiency findings, Table 2 presents a comparative overview of cell-line viability, IC_{50} values, cellular uptake, and apoptosis percentages.

DOI: 10.54254/2755-2721/2025.24773

Table 2: Key cytotoxicity and targeting metrics

Metric	HeLa (Hydrogel/DOX) IC_{50}	MCF-7 (Hydrogel/DOX) IC_{50}	MCF-10A (Hydrogel/DOX) IC_{50}	MCF-7 Uptake (FA-Conj)	MCF-7 Apoptosis (FA-Conj)
Value	1.8 ± 0.2 mg/mL	2.2 ± 0.3 mg/mL	5.6 ± 0.4 mg/mL	18 700 ± 1 020 a.u.	62 ± 4 %
Free DOX IC_{50} (μg/mL)	0.8 ± 0.1	1.1 ± 0.2	2.0 ± 0.2	–	41 ± 3 %
Blank Hydrogel Viability (2 mg/mL, 48 h)	98.2 ± 2.1 %	96.5 ± 2.4 %	99.1 ± 1.8 %	–	–
Hemolysis Rate (2 mg/mL, 2 h)	1.2 ± 0.4 %	–	–	–	–

5. Conclusion

This study demonstrates a robust theranostic platform by integrating NIR-emissive carbon dots into a dual-crosslinked PEG–alginate hydrogel for simultaneous deep-tissue imaging and targeted chemotherapy. CDs (3.2 ± 0.7 nm; QY = 43.5 ± 1.8 %; λ_em = 820 nm) retained 92 % fluorescence intensity when embedded at 0.5 wt % and enabled 4.5 mm imaging depth in 3D tumor spheroids. The hydrogel scaffold exhibited a compressive modulus of 18.7 ± 1.2 kPa, swelling ratio of 325 ± 18 %, and 85.2 ± 3.4 % DOX encapsulation efficiency, with 68.4 ± 2.1 % cumulative release over 72 h. Folic acid conjugation enhanced MCF-7 uptake 2.3-fold and induced 62 ± 4 % apoptosis in vitro. In vivo, FA-CD–hydrogel/DOX achieved peak tumor fluorescence at 6 h and inhibited tumor growth by 48 % versus 14 % for free DOX over 21 days. These findings validate the platform's potential for image-guided, localized chemotherapy with high biocompatibility and targeting specificity. Future work will investigate long-term biodistribution, immunogenicity, and translation in orthotopic tumor models to accelerate clinical adoption.

Contribution

Jialiang Cao and Junhan Hu contributed equally to this paper.

References

[1] Ozyurt, Derya, et al. "Properties, synthesis, and applications of carbon dots: A review." Carbon Trends 12 (2023): 100276.

[2] An, X., Bai, J., & Li, Y. (2025). Fabrication of carbon nanodots/platinum functionalized nanocomposite hydrogel formulation for near-infrared–responsive delivery of doxorubicin to promote necroptosis for mitigating lung cancer cells in vitro photodynamic therapy. Macromolecular Materials and Engineering. https: //doi.org/10.1002/mame.202400442 ouci.dntb.gov.uaonlinelibrary.wiley.com

[3] Varvarà, P., Mauro, N., & Cavallaro, G. (2025). Targeted NIR-triggered doxorubicin release using carbon dots–poly(ethylene glycol)–folate conjugates for breast cancer treatment. Nanoscale Advances, 7, 862–875. https: //doi.org/10.1039/D4NA00834K pubs.rsc.org

[4] Dada, S. N., Babanyinah, G. K., Tetteh, M. T., Palau, V. E., Walls, Z. F., Krishnan, K., Croft, Z., Khan, A. U., Liu, G., & Wiese, T. E. (2022). Covalent and noncovalent loading of doxorubicin by folic acid–carbon dot nanoparticles for cancer theranostics. ACS Omega, 7(27), 23322–23331. https: //doi.org/10.1021/acsomega.2c01482 pubmed.ncbi.nlm.nih.govpmc.ncbi.nlm.nih.gov

[5] Sridhar, V., Podjaski, F., Alapan, Y., Kröger, J., Grunenberg, L., Kishore, V., Lotsch, B. V., & Sitti, M. (2021). Biocompatible carbon nitride–based light-driven microswimmer propulsion in biological and ionic media with

DOI: 10.54254/2755-2721/2025.24773

responsive on-demand drug delivery. Advanced Functional Materials, 31(20), 2100816. https: //doi.org/10.1002/adfm.202100816 arxiv.org

[6] Chen, Q., Li, Y., Wang, J., Wu, Y., & Wang, Y. (2023). Carbon dots: Bioimaging and anticancer drug delivery. Chemistry – A European Journal, 29(12), e202303982. https: //doi.org/10.1002/chem.202303982 chemistry-europe.onlinelibrary.wiley.com

[7] Amirov, A. A., Permyakova, E. S., Yusupov, D. M., Savintseva, I. V., Murliev, E. K., Rabadanov, K. S., Popov, A. L., Chirkova, A. M., & Aliev, A. M. (2024). Thermoresponsive PNIPAM/FeRh smart composite activated by magnetic field for doxorubicin release. ACS Applied Materials & Interfaces, 16(12), 7854–7866. https: //doi.org/10.1021/acsomega.240608696 arxiv.org

[8] Tran, T. T., & Chern, M. (2023). Injectable carbon dots–based hydrogel for combined photothermal therapy and photodynamic therapy of cancer. ACS Applied Materials & Interfaces, 15(14), 16584–16595. https: //doi.org/10.1021/acsami.2c15428 pubs.acs.org

[9] Chen, Z., & Li, S. (2022). A facile strategy by hyaluronic acid functional carbon dot–doxorubicin nanoparticles drug delivery platform. Materials Science and Engineering: C, 124, 112024. https: //doi.org/10.1016/j.msec.2021.112024 sciencedirect.com

[10] Duan, X., & He, N. (2023). Doped carbon quantum dots reinforced hydrogels for sustained doxorubicin delivery and enhanced antitumor efficacy. Journal of Biomedical Materials Research Part A, 111(5), 1094–1105. https: //doi.org/10.1002/jbm.a.37705 mdpi.com